IEEE Access
Multidisciplinary | Rapid Review | Open Access Journal

Received 8 February 2024, accepted 25 March 2024, date of publication 28 March 2024, date of current version 4 April 2024.

Digital Object Identifier 10.1109/ACCESS.2024.3382711

RESEARCH ARTICLE

Radar Error Correlation Analysis Under the Simultaneous Observation of Double Targets

YUXIANG ZHOU, FAXING LU, QIUYANG DAI, AND JUNFEI XU
College of Weaponry Engineering, Naval University of Engineering, Qiaokou, Wuhan, Hubei 430000, China
Corresponding author: Faxing Lu (zyx19531@yeah.net)

ABSTRACT Radar error is a significant factor restricting the detection accuracy of radar. Improving the detection accuracy of radar is crucial to accurate target localization in an ocean environment. With a large amount of measured data, this paper presents the correlation analysis of radar errors, and gives the assumptions needed for radar error modeling. This provides theoretical support for calibrating the modeling method based on the radar error in the simultaneous observation of double targets. First, three error correction models were developed with constant, first-order, and second-order fitting methods, based on the origin and transfer of error in the radar system and the principles of error elimination and reduction in a cooperative platform. Subsequently, the advantages of using a cooperative platform including information sharing were used to detail the collection and preliminary processing of measured radar data as well as the establishment of datasets. Ultimately, the measured radar data were analyzed considering the random error of radar, the strategy for the selection of the optimal error correction model, and the detection error correlation of double targets. In particular, the second-order fitting model with the strongest azimuthal systematic error correlation calculated the root mean square error, which was 32.07% higher compared to the other two models. As revealed in the results of the error analysis, the random error of radar does not agree with the vector superposition characteristic, and it is strongly correlated with the system error of a single radar system that observes different targets within a short period. This provides a way for resolving some problems such as accurate target localization and time variance of error in the complex ocean environment.

INDEX TERMS Error correlation analysis, ship-borne radar, system error, error modeling.

I. INTRODUCTION

In the complex ocean environment, ship-borne radar may inevitably have some errors under the effect of such factors as performance indices, system design, radio refraction error, dynamic lag error, interference, and noise [1]. These errors can be classified into system and random errors [2]. A random error is normally attributed to the integrated effect of multiple uncertain factors, and it can be eliminated or reduced by filtering technology [3]. The system error is inherent, so that it cannot be easily eliminated by filtering technology. In a practical situation, a ship equipped with a high-precision real-time kinematic device is often taken as an auxiliary platform for beforehand calibration. While berthing at a dock, the parameters of system error are input into the radar system. However, this method cannot truly eliminate system errors of radar [4], [5]. When a ship-borne platform was maneuvering, its attitude error was always coupled with the sensor observation error. With the lapse of time and changes in the environment, the system error of radar would reappeared and became a complicated time-varying quantity because of the large number of wild values in the radar measurement information [6]. At this time, the system error of radar will severely undermine the radar's target localization accuracy. In order to improve radar detection accuracy and eliminate the effect of time-varying radar system errors, multi-platform joint target

The associate editor coordinating the review of this manuscript and approving it for publication was Huaqing Li.

localization [7], [8] and real-time error correction [9], [10], [11] has been adopted.

Compared with the localization of targets with a single platform, multi-platform cooperative localization features high accuracy, reliability, and robustness [12]. In order to resolve the real-time system error of radar in localization, many scholars have explored the multi-platform cooperative localization method. Shi et al. [13], [14] studied cooperative target tracking of unmanned aerial vehicles (UAVs) based on an aided beacon, and devised a multi-platform cooperative guidance law, so as to optimize the observed location of UAVs and improve the target localization accuracy of double UAVs. Fu et al. [15] analyzed a multi-platform formation cooperative localization algorithm from the perspective of information fusion, and improved the target cooperative localization accuracy by 36.9% and 23.5% for two typical mission scenarios, respectively. Zhou et al. [16] introduced the maximum likelihood method based on the measurement function, estimated and solved the systematic bias by interactive multi-model algorithm, which abated the distance information system error in the process of joint target localization.

The abovementioned scholars performed the physical or semi-physical simulation test to fully demonstrate the established methodological model, but they assumed that the system and random error were fixed in the simulation calculation, and that the random error agreed with the Gaussian distribution. This led to the effectiveness of the networked system being even inferior to the tracking measurement of a single radar. And the algorithm model used was too simple to be applied to real-time error estimation.

To eliminate the effect of time-varying systematic errors, the errors had to be introduced into the model of the linear error correction algorithm. Dai and Lu [17] put forward a target tracking algorithm for the theoretical elimination and reduction of sensor system error based on two platforms. A decoupled all-dimension augmentation model was built to achieve the real-time online estimation of target tracking. Huang et al. [18] proposed a double-order expansion Kalman filter error alignment algorithm based on the ECEF coordinate system, which responds to the problem that the joint dimension-expanding error alignment algorithm increases with dimension. However, the dimension expansion idea of this algorithm was only limited to the target stationary state without considering the effect of target maneuvering on the system error. Dong et al. [19] proposed a real-time error alignment algorithm for tracking target maneuvering conditions, which estimates the time-varying system error as part of the state vector in real time.

In the studies conducted by these scholars, the improved models and algorithms greatly reduced the computation time of data, improved the accuracy of calibration, and achieved real-time online estimation by combining system error vectors with state vectors using the idea of dimension expansion. However, their models were constructed on the assumption that the moving platform attitude and radar system errors were treated as a variable, and changed abruptly at the same time. Additionally, they still considered that the random error conformed to a Gaussian distribution. In the above-mentioned real-time error correction algorithms, it was simply assumed that the radar system error was a constant or changed abruptly with the moving platform attitude error, but such assumption was not verified in any test. Therefore, they could not give a satisfying description of the variance of the system error and random error of radar in the practical measurement.

In many existing algorithms, attention is often paid to the measurement error of a single radar system for a single target, or the joint error estimation of multiple sensors for different levels of filtering or modeling to reduce the random error and eliminate the system error. Nevertheless, the practical situation on the sea surface is often complicated and changing. A target is normally not isolated, and the location information of multiple groups of targets can be detected simultaneously in a single scan. Moreover, it is difficult to achieve the associated networking of multiple sensors, which required the construction of a high-speed data chain and the realization of fire-control-level transmission delays. A scan may gather the location information of multiple targets simultaneously [20]. As revealed in many practical efforts, if a single radar system is used to detect multiple targets simultaneously, and these targets are correlated to some extent, it can be approximately regarded that a source of the system error that remains unchanged during a cycle of scan [21], [22]. Therefore, distinguished from the previous mode of improving radar detection accuracy by optimizing the iterative co-location algorithm and real-time system error correction algorithm, this paper analyzed the correlation of errors, made use of it as a reference to eliminate the corresponding system errors, and opened up a new solution for the real-time correction of system errors.

This paper presents three system error fitting correction models with the practically measured data from a lake test to improve the accuracy of radar detection, scientifically verify the assumptions for building a real-time estimation model of radar system error, and address the real-time error correction of the radar system. In this way, the correlation law can be quickly introduced and promoted. Subsequently, a large amount of measured data is processed and analyzed for the collection and preliminary processing of radar data. The establishment and significance of three datasets are particularly elaborated. In the end, correlation analysis is introduced to separate the system error and random error of radar, sum up their regularities, verify when these models are applicable, and develop the reasonable model selection strategy. Theil's inequality coefficient and normalized Euclidean distance are borrowed to verify and analyze the error correlation of targets in two groups. Through the lake test and comparative analysis, this study will have a bright practical prospect since it delivers a new way to implement real-time error correction of the radar system and improve the accuracy of radar detection,

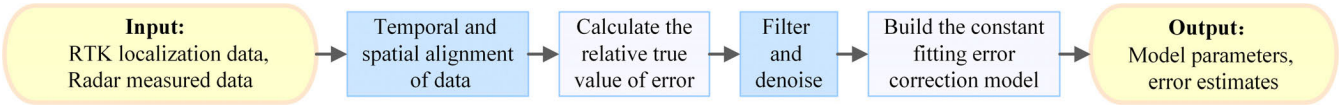

FIGURE 1. The constant fitting error correction process.

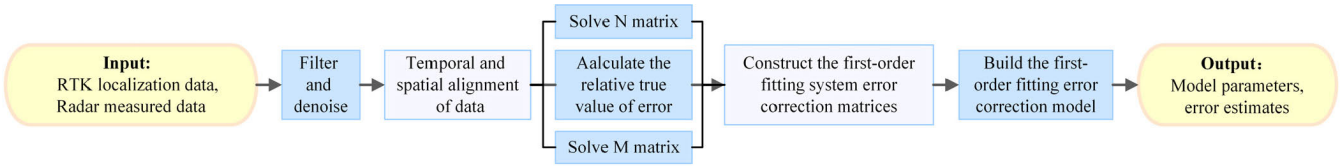

FIGURE 2. The first-order fitting error correction process.

and provides the support for the construction of a real-time radar error correction model.

II. RADAR SYSTEM ERROR CORRECTION MODELS

A radar error model may vary with the source of system error on which the researcher focuses. While performing the correlation analysis of radar error, it is necessary to first identify and classify the possible sources of error. Different types of radar error must be correspondingly quantified and assessed. A suitable mathematical model should be employed to illustrate the correlation of the value measured by radar and the actual value. In order to find a suitable and optimal model for correlation analysis, this paper presents three typical error correction models with constant, first-order, and second-order fitting methods. Moreover, the parameters were calculated in simulation for these models, so as to select a suitable and optimal model for subsequent analysis.

A. CONSTANT FITTING CORRECTION MODEL

System error is normally repetitive, one-directional, and measurable. On this basis, a constant fitting correction model is put forward. The algorithm follows the principle that the error of the target's location given by a real-time kinematic (RTK) device is taken as the relative true value of such error. Moreover, the error of the target's position measured by the navigation radar is taken as the measured value. The influence of external environment and conditions on radar is ignored. The position given by RTK has no system error or random error. The measured value is corrected by statistical method.

The constant fitting error correction process is as follows:

Following the principles of the algorithm, the error correction model was defined by (1):

$$\begin{cases} R_r = R_m + R_0 \\ A_r = A_m + A_0 \\ E_r = E_m + E_0 \end{cases} \tag{1}$$

Equation (1) was transformed to obtain the constant fitting system error correction equation (the process is presented in APPENDIX A):

$$\begin{cases} R_0 = \dfrac{1}{n}\displaystyle\sum_{i=1}^{n} \Delta R_i \\ A_0 = \dfrac{1}{n}\displaystyle\sum_{i=1}^{n} \Delta A_i \\ E_0 = \dfrac{1}{n}\displaystyle\sum_{i=1}^{n} \Delta E_i \end{cases} \tag{2}$$

where R_0, A_0, and E_0 are the range-,azimuth-, and the elevation-zero set constants, R_r, A_r, and E_r are the rectified range, azimuth and elevation values, R_m, A_m, and E_m are measured values for range, azimuth and elevation, respectively.

B. FIRST-ORDER FITTING CORRECTION MODEL

Navigation radar is affected by a wide variety of external and internal factors. For this reason, some sources of error were identified, e.g., range-, azimuth- and elevation-zero set constants, azimuth-elevation axis non-orthogonality, radar antenna seat out-of-level, and azimuth-elevation optical-electrical axis non-parallelism. On this basis, a first-order fitting error correction model was constructed [23].

The principles of the algorithm are as follows: the temporal and spatial alignment of data was first performed to calculate the relative true value of error. In the algorithm, the source of range error was not taken into account. Therefore, the first-order modeling of the range error was carried out in the same process of the constant fitting model. Subsequently, the azimuth and elevation errors were calculated by the polynomial with undefined parameters for the azimuth and elevation errors in the first-order error correction model. With the least squares method, the measured data matrix was used to calculate the parameters of the polynomial. The values of variables for each error were inversely estimated. After all, the original data measured by radar were substituted into the model to calculate the system error after correction in the model. The accuracy of the model could be therefore determined.

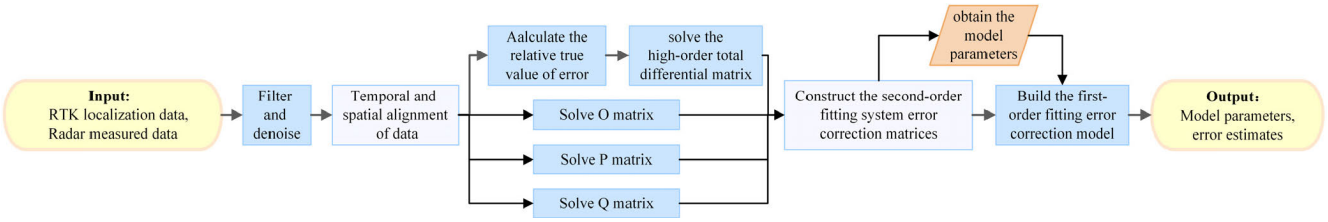

FIGURE 3. The second-order fitting error correction process.

Following the principles of the algorithm, the error correction model was defined by (3):

$$\begin{cases} R_r = R_m + R_0 \\ A_r = A_m + A_0 + \theta_m \sin(A_m - A_{\max}) \tan E_m \\ \qquad +\delta_m \tan E_m + V_{az} \sec E_m \\ E_r = E_m + E_0 + \theta_m \cos(A_m - A_{\max}) + V_e \end{cases} \tag{3}$$

Based on the principles of the least squares method, equation (3) was transformed to obtain the first-order fitting system error correction equation (see APPENDIX A for the process of derivation, the actual meanings of parameters and the comparison of parameters):

$$\begin{cases} R_0 = \dfrac{1}{k} \displaystyle\sum_{i=1}^{k} \Delta R_i \\ X = \left(M^T M\right)^{-1} M^T \Delta A' \\ Y = \left(N^T N\right)^{-1} N^T \Delta E' \end{cases} \tag{4}$$

where V_{az} is the azimuth optical-electrical axis non-parallelism angle, δ_m is the azimuth-elevation axis non-orthogonality angle, $A_{\max}$ is the azimuth angle of the maximum out-of-level angle, V_e is the elevation optical-electrical axis non-parallelism angle.

C. SECOND-ORDER FITTING CORRECTION MODEL

System error was further divided considering the practical connection, regulation, calibration, and proofreading of radar. Some new sources of error were identified to introduce axis system, time, radio wave refraction, and dynamic lag types of error. On this basis, a radar system error model with the second-order model coefficients was constructed and regarded as the second-order fitting error correction model [19].

Following the principles of the algorithm, the error correction model is defined by (5), as shown at the bottom of the next page.

The undefined coefficients were estimated by the least squares method. After transformation, the second-order fitting system error correction equation was derived as follows (6) (see APPENDIX A for the process of derivation, the actual meanings of parameters and the comparison of parameters):

$$\begin{cases} A = (O^T O)^{-1} O^T \Delta R' \\ B = (P^T P)^{-1} P^T \Delta A' \\ C = (Q^T Q)^{-1} Q^T \Delta E' \end{cases} \tag{6}$$

where Δt_1 is the timing error, Δt_2 is the time delay of spatial propagation, K_c, K_f, K_v, K_a, and K_j are the radial acceleration, radial jerk, azimuth velocity azimuth acceleration, azimuth jerk dynamic lag error coefficients, respectively, K_b is the optical axis elevation non-orthogonality, K_z is the azimuth component of optical-electrical non-parallelism, K_n is the elevation component of optical-electrical non-parallelism, K_g is the weight distortion coefficient, θ_m is the maximum out-of-level angle, A_m is the direction of the maximum out-of-level inclination, λ is the azimuth-elevation axis non-orthogonality, α is the range radio wave refraction correction coefficient, β is the elevation radio wave refraction correction coefficient, and N_j is the random error.

III. VERIFICATION TEST

A lake test was carried out for field measurement to improve the accuracy of the real-time radar correction model, verify the preconditions for the construction of the radar error model based on the cooperative platform, and analyze the system error and random error of radar. The actual data were collected from the simultaneous observation of double targets with a single radar system, and kept for subsequent analysis and application.

In this section, external devices were used to gather the original data of radar, and perform the temporal and spatial alignment. The aligned data of targets and the data from the cooperative platform were analyzed and processed to generate the datasets needed to build the error models. The parameters of the error fitting correction models were solved.

A. DESIGN OF EXPERIMENTS

In order to analyze the correlation between the simultaneous observation of two targets by a single radar, we carried out a radar measurement experiment at Honglian Lake in Hubei Province. The YAR28(N) small-target maritime cyber radar mounted on the swing platform was used to detect and locate the two simulated targets as well as to complete data logging. The two simulated targets were speedboats fitted with corner reflectors with a calculated single-boat equivalent RCS

FIGURE 4. Data alignment process.

mean value of 38.75 dBsm, which were 34 metres in length, 6.7 metres in width, and 7.7 metres in height. The radar was positioned at the origin of the coordinates. According to the engineering practice, the radar sampling interval T was set to 1 second, the radial distance observation accuracy σ_r was set to 50 metres, and the azimuth observation accuracy σ_θ was set to 0.5°. Fig. 4 shows a satellite map of the test area, indicating the radar and the range of activity of the two targets. The movements and trajectories of the two targets were pre-determined, ensuring that they traverse within a feasible area along a planned path while continuously logging radar detection data.

B. COLLECTION OF RADAR DATA

In this paper, test data were mainly collected from a YAR28(N) small-target maritime cyber radar. Fig. 5(a) shows a scene on shore where the installation and commissioning of the radar system was carried out. The radar system was mainly composed of four device units including an antenna and receiver unit, display unit, main computer unit, and keyboard unit. The transmission frequency was X-band. The antenna used the horizontal polarization waveguide slot system. The rotational speed was 24 rpm. In order to measure the location and attitude of radar, some input devices were also needed to provide external parameters including an NES-1008 AIS/GPS electronic chart instrument and a BD-MGI680 integrated navigation system. Figs. 5(b) and 5(c) show the relative positions of the two target ships with angular reflectors and the radar used in the experiment.

First, the original data message directly gathered from the radar processor unit could not be simply processed due to different protocols of the input and output interfaces. Fig. 5(d) shows the HMI (Human Machine Interface) of the radar. The message must be preliminarily analyzed. Subsequently, serial communication software was designed for the real-time display of inertial navigation data in the radar and integrated navigation system. The real-time data of radar's target detection could be obtained. Next, the radar's target tracking message was analyzed to extract the information of target's location including time stamp, target distance, azimuth, and elevation. The message contained RAOSD own ship status data statements, RARSD radar system status data statements, and RATTM target tracking statements. Using the datagram form of RATTM, the information including UTC time stamp, distance, azimuth, and elevation was collected to obtain the target point trace data. In the end, the interacting multiple model algorithm based on Kalman filter was introduced to construct the filter [24], [25], [26]. The algorithm can be used to eliminate and reduce the sensor random error and the attitude random error. Therefore, the error in the observation of sea targets can be achieved in a fast and accurate way.

C. TEMPORAL AND SPATIAL ALIGNMENT OF RADAR DATA

Effective information must be extracted from a large amount of measured data to analyze the error of the radar system, and then the regularity of its variation needs to be identified. The data rate of a radar system depends on its scan cycle. Data analysis and modeling must be carried out in a unified way. Therefore, the data of radar coordinates measured at different times must be temporally aligned before building an error correction model. The goal is to eliminate time warp, ensure data continuity, and improve model accuracy. The algorithm presented in Fig. 6 was devised for conducting temporal and spatial alignment. Two alignment methods were available for different scenarios. If the point traces of data were sparse, and the data at adjacent time points did not vary dramatically, the nearest neighbor interpolation method could be adopted. Otherwise, the linear interpolation method was selected.

D. ESTABLISHMENT OF DATASETS

For the real-time estimation of radar system error, efforts must be made to overcome the massive computation time

$$\begin{cases} R_r = R_m + R_0 + \Delta t_1 \dot{R} + \Delta t_2 \dot{R} + \alpha \sec E + \dfrac{\ddot{R}}{K_c} + \dfrac{\dddot{R}}{K_f} + N_{R_m} \\ A_r = A_m + A_0 + \Delta t_1 \dot{A} + \Delta t_2 \dot{A} + \theta_m \sin(A_m - A_{\max}) \tan E_m + \lambda \tan E_m + (K_Z + K_b) \sec E_m + \dfrac{\dot{A}}{K_v} + \dfrac{\ddot{A}}{K_a} + \dfrac{\dddot{A}}{K_j} + N_{A_m} \\ E_r = E_m + E_0 + \Delta t_1 \dot{E} + \Delta t_2 \dot{E} + \theta_m \cos(A_m - A_{\max}) + K_g \cos E_m + K_n + \beta \cot E + \dfrac{\dot{E}}{K_v} + \dfrac{\ddot{E}}{K_a} + \dfrac{\dddot{E}}{K_j} + N_{E_m} \end{cases} \tag{5}$$

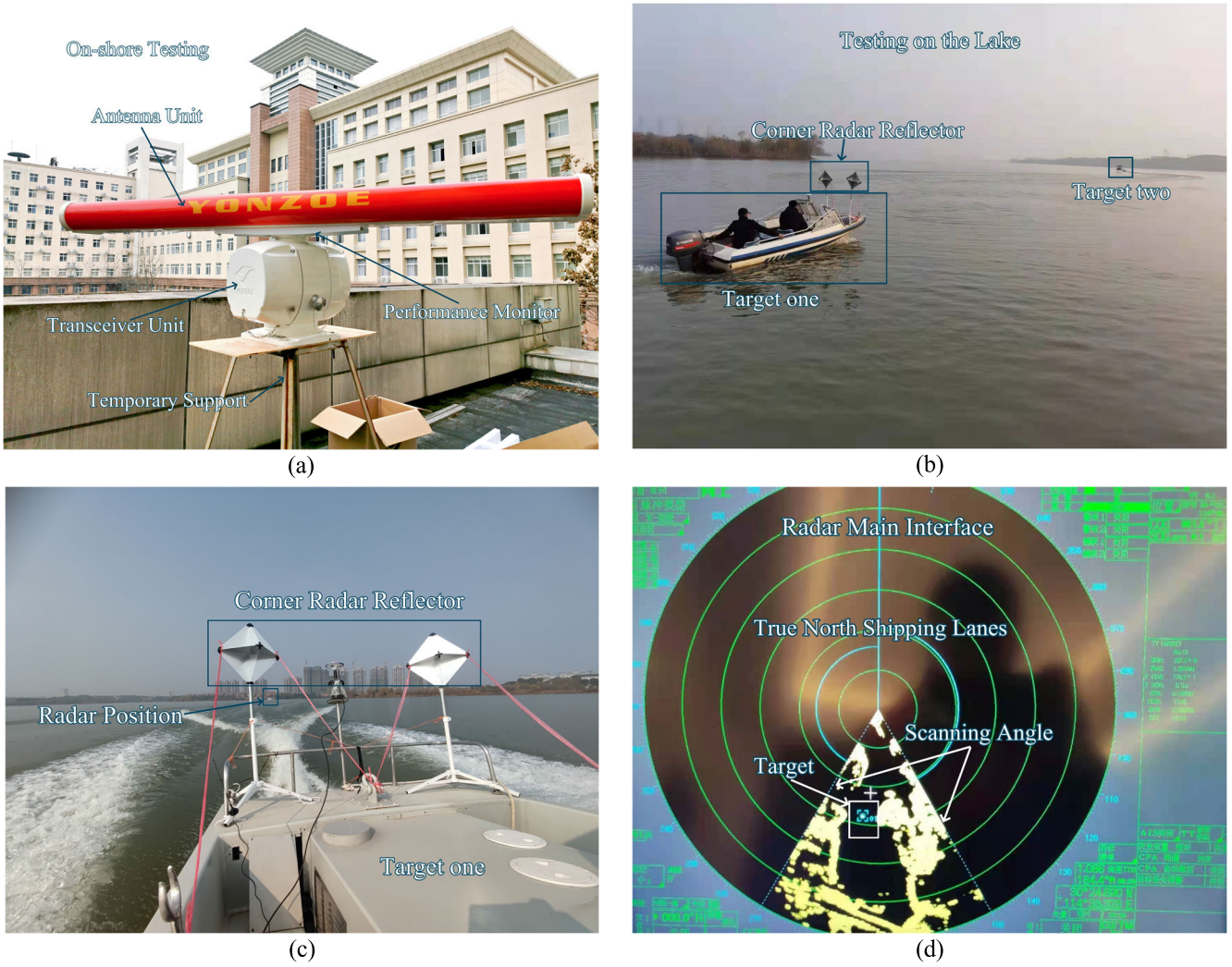

FIGURE 5. Experimental validation of radar systems. (a) On-shore Testing; (b) Testing on the lake from the shore view; (c) Testing on the lake from the target boat view; (d) Radar main interface.

needed while guaranteeing high accuracy. An accurate model must be constructed for correction. In this study, the parameters of the error fitting correction models were solved to analyze the radar system error, and revealing the regularity of its variation in different motion states of the targets. The datasets were established in the process as given in Fig. 7.

The aligned point trace data were processed in categories. The trace plots were used to select the segments of different motion states of the targets. These segments were eventually connected to generate three datasets (see Figs. 8 and 9 for trace plots) for subsequent analysis. Among them, dataset 1 is the point trace dataset of the targets in rectilinear motion, dataset 2 is the point trace dataset of the cooperative platform in rectilinear motion, in addition, dataset 3 is the point trace dataset of double targets in rectilinear motion (see APPENDIX B for dataset processing).

IV. ERROR ANALYSIS

A. RANDOM ERROR OF RADAR DETECTION

As discussed above, the interactive multiple model filtering algorithm based on a Kalman filter was adopted to reduce the influence of random error and filter the random error in the originally measured trajectories. The data simultaneously measured by the radar system for the targets and the cooperative platform were filtered and calculated for modeling. The differences between the errors were used to determine the range and azimuth error differences. Currently existing real-time error estimation methods assume that random error is a constant or subject to a Gaussian distribution at the time of modeling. However, such an assumption is not valid as revealed in the comparative analysis of massive test data in this paper. In Figs. 10 and 11, the first one of each figure presents the range and azimuth errors, and the second one contains their differences in dataset 3 (which is formed by datasets 1 and 2, including the first 1000 pieces of data

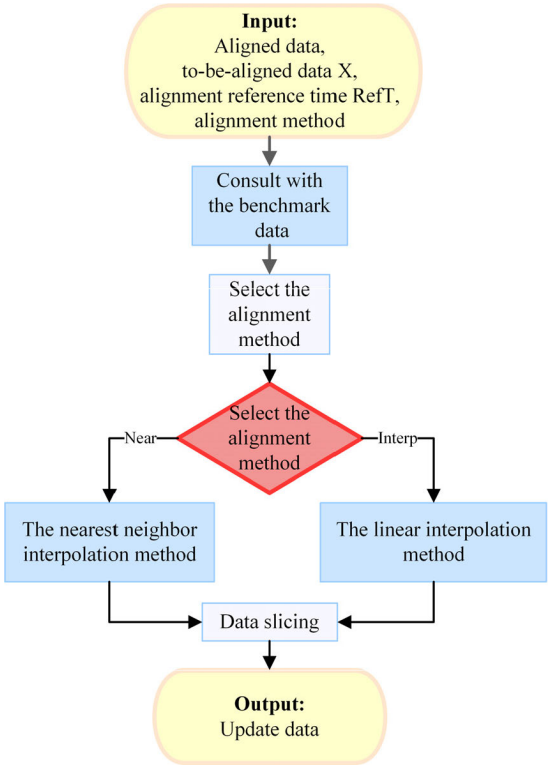

FIGURE 6. Data alignment process.

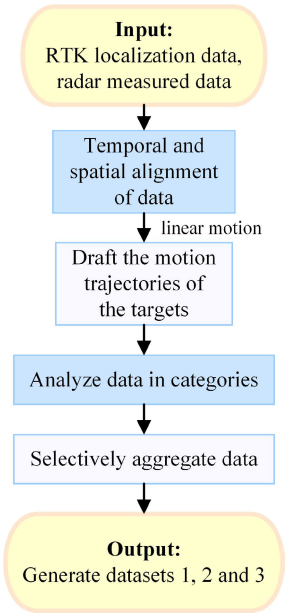

FIGURE 7. Dataset creation process.

captured from dataset 1 and the second 1000 pieces from dataset 2).

As shown in Fig. 10, the original range error fluctuates between −17.5 m and 7.5 m, the random error amplitude is approximately 25 m, the range error difference varies from −15 m to 10 m, and the random error amplitude is approximately 25 m. In Fig. 11, the original azimuth error

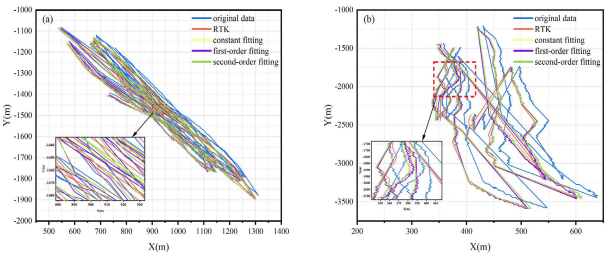

FIGURE 8. Trace plot of targets in rectilinear motion. (a) Datasets 1; (b) Datasets 2.

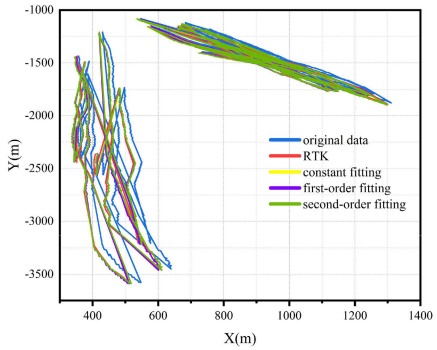

FIGURE 9. Trace plot of double targets in rectilinear motion (dataset 3).

varies from 0.1° to 0.9°, the random error amplitude is around 0.8°, the azimuth error difference varies from −0.3° to 0.4°, and the random error amplitude is around 0.7°. It was assumed that the two targets in simultaneous observation have the same system error. After comparing the error differences before and after filtering, it was found that the random error amplitude decreased and had no vector superposition when a single radar system tracks and measures two targets at the same time. Meanwhile, it was also noticed that the mean value of errors approximately had a fixed offset. The random error offset of range was 5 m, while the random error offset of azimuth was 0.45°. In other words, there was still a residual system error after filtering.

B. SELECTION OF THE OPTIMAL ERROR CORRECTION MODEL

In order to vividly reflect the error characteristics of the radar, some characteristic parameters were selected including expected errors (see Table 1), variances (see Table 2), and root mean square errors (see Table 3). The modeling analysis results of test datasets were evaluated. A strategy was developed to select the optimal error correction model.

The mean values of error were not affected by filtering and correction. As for the radar system, the expected system error of range is approximately −5.5 m, and the expected system error of azimuth is 0.009°.

After filtering and correction, the variance of the system error decreased significantly and tended to be zero. This indicates that all three fitting correction models have unbiased estimation.

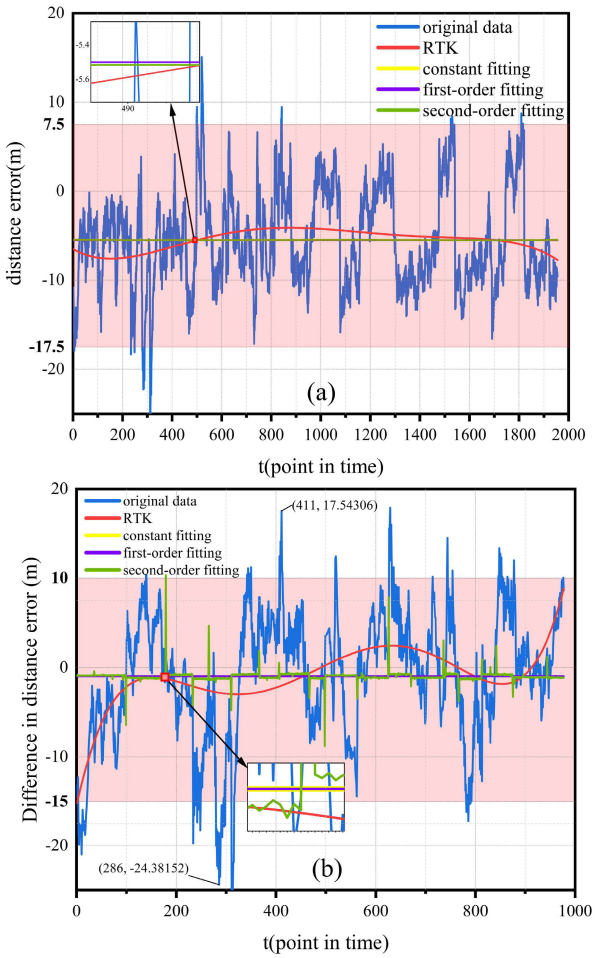

FIGURE 10. Random error analysis of range.

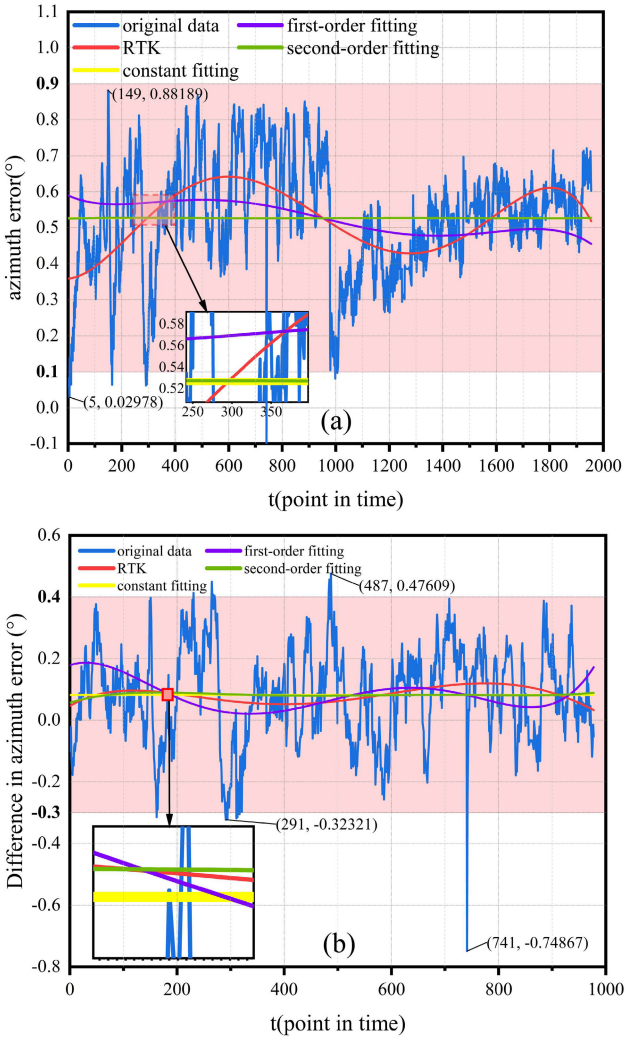

FIGURE 11. Random error analysis of azimuth.

In the table, the bold data are the lowest root mean square errors in the respective columns.

Therefore, the second-order error model should be selected for range error correction, and the first-order model for azimuth error correction while measuring the targets in rectilinear motion.

Based on the calculation data and the range and azimuth error diagrams of the targets in rectilinear motion, the following strategy is proposed for the selection of the optimal error correction model:

(i) During the test, frequent maneuvering should be avoided as much as possible. The target engages in uniform rectilinear motion to improve measurement accuracy.

(ii) In the processing of test data, a second-order system error fitting correction model should be selected for the correction of range error, and a first-order system error fitting correction model for the correction of azimuth error.

C. CORRELATION ANALYSIS OF ERRORS IN THE DETECTION OF DOUBLE TARGETS

When a single radar system is used for the simultaneous detection of double targets, it is exposed to various problems such as a complicated environment and unknown correlation of errors. Therefore, correlation analysis was carried out with the extracted error parameters. Theil's inequality coefficient (TIC) and normalized Euclidean distance were adopted to

TABLE 1. Mean values of error.

Error type	Range	Azimuth
Original error	-5.499	0.009
Residual error after filtering	-5.499	0.009
Constant fitting of targets	-5.500	0.009
First-order fitting of targets	-5.500	0.009
Second-order fitting of targets	-5.499	0.009

TABLE 2. Variances of error.

Error type	Range	Azimuth
Original error	30.847	0.000
Residual error after filtering	1.198	0.000
Constant fitting of targets	0.000	0.000
First-order fitting of targets	0.000	0.000
Second-order fitting of targets	0.000	0.000

TABLE 3. Root mean square errors.

Error type	Range	Azimuth
Constant fitting of targets	5.7879	0.002059
First-order fitting of targets	5.7879	**0.001559**
Second-order fitting of targets	**5.7835**	0.002055

TABLE 4. Theil's inequality coefficients.

Error type	Range	Azimuth
Constant fitting of targets	0.088	0.0784
First-order fitting of targets	0.088	**0.0781**
Second-order fitting of targets	**0.087**	0.0893

verify the correlation of two targets observed in the same period.

1) THEIL'S INEQUALITY COEFFICIENT

In the TIC method, a scalar function was created for the system errors of two targets under the same environmental conditions, so as to qualitatively measure the consistency and dynamic correlation of two datasets. This method does not require the independence and normality of data sequence, so that it is characterized by simple implementation and low computation time. Therefore, it provides an effective way to verify dynamic correlation.

It is assumed that $\{x_n\}$ and $\{y_n\}$ are the output sequences of the first target and the cooperative platform, respectively, where n = 1, 2...N, and N is the length of data sequence:

$$TIC = \frac{\sqrt{\frac{1}{N}\sum_{n=1}^{N}(x_n - y_n)^2}}{\sqrt{\frac{1}{N}\sum_{n=1}^{N}x_n^2} + \sqrt{\frac{1}{N}\sum_{n=1}^{N}y_n^2}} \tag{7}$$

where N is the number of data points after temporal and spatial alignment, x_n is the normalized error of the target 1, including errors at all orders, and y_n is the normalized error of the target 2, including errors at all orders.

By (7), it was found that TIC was between 0 and 1. The lower the TIC, the better correlation of $\{x_n\}$ and $\{y_n\}$. When TIC is close to 1, these two are significantly different. The two error data sequences were substituted into the equation to solve for TIC. As shown in Table 4, TIC was always lower than 0.3, so that it is normally believed that no significant difference exists between the two data sequences. In other words, the data are well correlated. Hence, the short-term system errors of the radar system in the observation of different targets are strongly correlated. This provides the practical basis for radar system error correction based on a cooperative platform.

TABLE 5. Normalized euclidean distances.

Error type	Range	r	Azimuth	r
Constant fitting of targets	44.181	0.694	44.181	0.694
First-order fitting of targets	44.181	0.694	**37.922**	**0.725**
Second-order fitting of targets	**38.592**	**0.722**	38.773	0.721

TABLE 6. Improvement of correlation coefficients.

Model type	Range	Enhancement	Azimuth	Enhancement
Constant fitting of targets	5.7879	0	0.002059	0
First-order fitting of targets	5.7879	0	**0.001559**	**+32.07%**
Second-order fitting of targets	**5.7835**	**+0.56%**	0.002055	+0.19%

2) NORMALIZED EUCLIDEAN DISTANCE

The normalized Euclidean distance is an improvement of the simple Euclidean distance. In this method, components are normalized for equal mean variance prior to computation. This can reflect the system error difference of a single radar system in the simultaneous observation of two targets, and represent the level of correlation between them. The specific equation is as follows:

$$distance = \sqrt{\sum_{i=1}^{N}\frac{(u_i - v_i)^2}{V_{x_i}}} \tag{8}$$

where N is the number of data points after temporal and spatial alignment, u_i is the normalized error of the target 1, including errors at all orders, v_i is the normalized error of the target 2, including errors at all orders, V_{x_i} is the variance of each target's error, *distance* is the normalized Euclidean distance.

According to the definitions, it is believed that the normalized Euclidean distance is negatively correlated with the error correlation. The calculated Euclidean distance was normalized by (9) to clearly demonstrate the relationship between the normalized Euclidean distance and the system error correlation.

$$r = 1 - \frac{distance}{100} \tag{9}$$

where *distance* is the normalized Euclidean distance, and r is the correlation coefficient.

Based on the calculated results in Table 5, the system errors of two targets were different when a single radar system was used to detect two targets simultaneously, but they were strongly correlated. Different error models lead to different levels of correlation with regard to range error and azimuth error. Table 6 below compared the relationship between the correlation coefficients and the systematic errors, and it can be shown that the distance systematic error calculated by the second-order system error fitting correction model with

the strongest correlation of the range error was the smallest, and the first-order system error fitting correction model with the strongest correlation of the azimuth error calculates the smallest orientation systematic error.

V. CONCLUSION

This paper presents a closed loop of data flow from data collection, data transmission, data correlation analysis and data modeling to error simulation. A large amount of measured data obtained from the theoretical analysis and lake test were processed and analyzed to draw the following conclusions:

(i)The random error of radar does not conform to a Gaussian distribution. The vector superposition of the random error in a single platform's target detection does not vary significantly, and it is not doubled. The mean value of error is approximately an offset in a fixed direction.

(ii)The system error of radar is a time-varying quantity affected by the motion state and attitude of the platform, motion state of targets, localization accuracy of the cooperative platform, and environmental changes.

(iii)In the processing of original data, a second-order system error fitting correction model should be selected for the correction of range error, and the first-order system error fitting correction model should be used for the correction of azimuth error.

(iv)When a single radar system is used for the detection of two targets, the system errors caused by two targets are different, but are strongly correlated within a short period. The most correlated systematic error fitting correction model has the highest accuracy. The related sources of error can be analyzed to rectify the trajectory of the key observed object, so as to improve the accuracy of tracking and measurement. The model selection strategy can be developed by calculating the correlation of systematic errors after model correction.

However, due to the limitation of experimental conditions, this paper did not carry out more simulation calculations of the error correction model, and the established dataset only intercepted the measured data of the target's linear motion part. In the future, we will develop the pertinent interface program in alignment with the software copyright submitted by the project team, tailored to the research topic of radar error correction. Additionally, we aim to establish a real-time radar detection system by analyzing the error correlation within the radar system and selecting the most suitable error correction model.

In this paper, correlation analysis of system error was carried out to realize the collection and preliminary processing of the radar's original data. The parameters of the cooperative platform were obtained to analyze the correlation of the targets and the cooperative platform. Three error fitting correction models were built to provide the strategy for the selection of the optimal error model. This presents a new approach for studying the real-time correction of the radar's system error and improving the accuracy of radar detection, and also provides the support for the real-time error calibration model for radar data based on the cooperative platform.

On the basis of the radar target system error correlation law discovered in this paper, the correlation between the targets of one single radar when detecting multiple batches of targets at the same time will be researched, and the radar system error correction algorithm based on the error correlation analysis will be explored.

APPENDIX A
DERIVATION OF THREE FITTING CORRECTION MODELS AND THEIR PARAMETERS

A. CONSTANT FITTING CORRECTION MODEL

Following the principles of the algorithm, the error correction model was defined by (a1):

$$\begin{cases} R_r = R_m + R_0 \\ A_r = A_m + A_0 \\ E_r = E_m + E_0 \end{cases} \tag{a1}$$

Equation (a2) was transformed to obtain:

$$\begin{cases} \Delta R = R_r - R_m = R_0 \\ \Delta A = A_r - A_m = A_0 \\ \Delta E = E_r - E_m = E_0 \end{cases} \tag{a2}$$

Then, let:

$$\Delta R = \begin{bmatrix} R_{r,1} - R_{m,1} \\ R_{r,2} - R_{m,2} \\ \vdots \\ R_{r,n} - R_{m,n} \end{bmatrix}, \Delta A = \begin{bmatrix} A_{r,1} - A_{m,1} \\ A_{r,2} - A_{m,2} \\ \vdots \\ A_{r,n} - A_{m,n} \end{bmatrix},$$
$$\Delta E = \begin{bmatrix} E_{r,1} - E_{m,1} \\ E_{r,2} - E_{m,2} \\ \vdots \\ E_{r,n} - E_{m,n} \end{bmatrix} \tag{a3}$$

The constant fitting system error correction equation was obtained as follows:

$$\begin{cases} R_0 = \dfrac{1}{n}\displaystyle\sum_{i=1}^{n} \Delta R_i \\ A_0 = \dfrac{1}{n}\displaystyle\sum_{i=1}^{n} \Delta A_i \\ E_0 = \dfrac{1}{n}\displaystyle\sum_{i=1}^{n} \Delta E_i \end{cases} \tag{a4}$$

B. FIRST-ORDER FITTING CORRECTION MODEL

Following the principles of the algorithm, the error correction model was defined by (a5):

$$\begin{cases} R_r = R_m + R_0 \\ A_r = A_m + A_0 + \theta_m \sin(A_m - A_{\max}) \tan E_m \\ \qquad +\delta_m \tan E_m + V_{az} \sec E_m \\ E_r = E_m + E_0 + \theta_m \cos(A_m - A_{\max}) + V_e \end{cases} \tag{a5}$$

TABLE 7. Original and actual parameters in first-order fitting.

Original parameter	Actual parameter	Original parameter	Actual parameter
x_0	A_0	y_0	E_0+V_e
x_1	$\theta_m \cos A_{\max}$	y_1	$\theta_m \cos A_{\max}$
x_2	$\theta_m \sin A_{\max}$	y_2	$\theta_m \sin A_{\max}$
x_3	δ_m		
x_4	V_{az}		

Equation (a6) is transformed to obtain:

$$\begin{cases} \Delta R = R_r - R_m = R_0 \\ \Delta A = A_r - A_m = x_0 + \sin A_m \tan(E_m)x_1 \\ \quad - \cos A_m \tan(E_m)x_2 \\ \quad + \tan(E_m)x_3 + \sec(E_m)x_4 \\ \Delta E = E_r - E_m = y_0 + \cos(A_m)y_1 + \sin(A_m)y_2 \end{cases} \tag{a6}$$

Then, let:

$$\Delta R = \begin{bmatrix} R_{r,1} - R_{m,1} \\ R_{r,2} - R_{m,2} \\ \vdots \\ R_{r,n} - R_{m,n} \end{bmatrix}, \Delta A = \begin{bmatrix} A_{r,1} - A_{m,1} \\ A_{r,2} - A_{m,2} \\ \vdots \\ A_{r,n} - A_{m,n} \end{bmatrix},$$
$$\Delta E = \begin{bmatrix} E_{r,1} - E_{m,1} \\ E_{r,2} - E_{m,2} \\ \vdots \\ E_{r,n} - E_{m,n} \end{bmatrix} \tag{a7}$$
$$X = \begin{bmatrix} x_0 \\ x_1 \\ x_2 \\ x_3 \\ x_4 \end{bmatrix}, Y = \begin{bmatrix} y_0 \\ y_1 \\ y_2 \end{bmatrix}, N = \begin{bmatrix} 1 & \cos A_{m,1} & \sin A_{m,1} \\ 1 & \cos A_{m,2} & \sin A_{m,2} \\ \vdots & \vdots & \vdots \\ 1 & \cos A_{m,k} & \sin A_{m,k} \end{bmatrix} \tag{a8}$$

With the least squares method, Equation (a9), as shown at the top of the next page, was transformed to obtain the first-order fitting system error correction equation as follows:

$$\begin{cases} R_0 = \dfrac{1}{k}\sum_{i=1}^{k} \Delta R_i \\ X = \left(M^T M\right)^{-1} M^T \Delta A' \\ Y = \left(N^T N\right)^{-1} N^T \Delta E' \end{cases} \tag{a10}$$

Equation (a10) was solved to obtain the original parameter matrix of the first-order fitting system error model. Equations (a5)-(a9) ware substituted into (a10). According to their definitions in matrices X and Y, the actual parameters of the model were obtained for modeling. The actual meanings of these parameters in the model are presented in Table 7:

TABLE 8. Original and actual parameters in second -order fitting.

Original parameter	Actual parameter	Original parameter	Actual parameter	Original parameter	Actual parameter
a_0	R_0	β_0	A_0	c_0	E_0
a_1	$\Delta t_1 + \Delta t_2$	β_1	$\Delta t_1 + \Delta t_2 + \dfrac{1}{K_v}$	c_1	$\Delta t_1 + \Delta t_2 + \dfrac{1}{K_v}$
a_2	∂	β_2	$\dfrac{1}{K_a}$	c_2	$\dfrac{1}{K_a}$
		β_3	$\theta_m \cos A_{\max}$	c_3	$-\theta_m \sin A_{\max}$
		β_4	$\theta_m \sin A_{\max}$	c_4	$\theta_m \cos A_{\max}$
		β_5	λ	c_5	K_g
		β_6	$K_z + K_b$	c_6	β

C. SECOND-ORDER FITTING CORRECTION MODEL

Following the principles of the algorithm, the error correction model was defined by (a11), as shown at the top of the next page.

The measured data of navigation radar and the relative true value of error were substituted into the error correction model defined by (a11) to solve for the undefined parameters.

Equation (a11) was transformed to obtain (a12), as shown at the top of the next page.

Then, let:

$$\Delta R = \begin{bmatrix} R_{r,1} - R_{m,1} \\ R_{r,2} - R_{m,2} \\ \vdots \\ R_{r,n} - R_{m,n} \end{bmatrix}, \Delta A = \begin{bmatrix} A_{r,1} - A_{m,1} \\ A_{r,2} - A_{m,2} \\ \vdots \\ A_{r,n} - A_{m,n} \end{bmatrix},$$
$$\Delta E = \begin{bmatrix} E_{r,1} - E_{m,1} \\ E_{r,2} - E_{m,2} \\ \vdots \\ E_{r,n} - E_{m,n} \end{bmatrix} \tag{a13}$$
$$A = \begin{bmatrix} a_0 \\ a_1 \\ a_2 \end{bmatrix}, B = \begin{bmatrix} b_0 \\ b_1 \\ b_2 \\ b_3 \\ b_4 \\ b_5 \\ b_6 \end{bmatrix}, C = \begin{bmatrix} c_0 \\ c_1 \\ c_2 \\ c_3 \\ c_4 \\ c_5 \\ c_6 \end{bmatrix},$$
$$O = \begin{bmatrix} 1 & \dot{R}_{j,1} & \sec E_{j,1} \\ 1 & \dot{R}_{j,2} & \sec E_{j,2} \\ \vdots & \vdots & \vdots \\ 1 & \dot{R}_{j,k} & \sec E_{j,m} \end{bmatrix} \tag{a14}$$
$$Q = \begin{bmatrix} 1 & \dot{E}_{j,1} & \ddot{E}_{j,1} & \sin A_{j,1} & \cos A_{j,1} & \cos E_{j,1} & \cot E_{j,1} \\ 1 & \dot{E}_{j,2} & \ddot{E}_{j,2} & \sin A_{j,2} & \cos A_{j,2} & \cos E_{j,2} & \cot E_{j,2} \\ \vdots & \vdots & \vdots & \vdots & \vdots & \vdots & \vdots \\ 1 & \dot{E}_{j,k} & \ddot{E}_{j,k} & \sin A_{j,k} & \cos A_{j,k} & \cos E_{j,k} & \cot E_{j,k} \end{bmatrix} \tag{a15}$$

$$M = \begin{bmatrix} 1 & \sin A_{m,1} \tan E_{m,1} & -\cos A_{m,1} \tan E_{m,1} & \tan E_{m,1} & \sec E_{m,1} \\ 1 & \sin A_{m,2} \tan E_{m,2} & -\cos A_{m,2} \tan E_{m,2} & \tan E_{m,2} & \sec E_{m,2} \\ \vdots & \vdots & \vdots & \vdots & \vdots \\ 1 & \sin A_{m,k} \tan E_{m,k} & -\cos A_{m,k} \tan E_{m,k} & \tan E_{m,k} & \sec E_{m,k} \end{bmatrix} \tag{a9}$$

$$\begin{cases} R_r = R_m + R_0 + \Delta t_1 \dot{R} + \Delta t_2 \dot{R} + \alpha \sec E + \dfrac{\ddot{R}}{K_c} + \dfrac{\dddot{R}}{K_f} + N_{R_m} \\ A_r = A_m + A_0 + \Delta t_1 \dot{A} + \Delta t_2 \dot{A} + \theta_m \sin(A_m - A_{\max}) \tan E_m + \lambda \tan E_m + (K_Z + K_b) \sec E_m + \dfrac{\dot{A}}{K_v} + \dfrac{\ddot{A}}{K_a} + \dfrac{\dddot{A}}{K_j} + N_{A_m} \\ E_r = E_m + E_0 + \Delta t_1 \dot{E} + \Delta t_2 \dot{E} + \theta_m \cos(A_m - A_{\max}) + K_g \cos E_m + K_n + \beta \cot E + \dfrac{\dot{E}}{K_v} + \dfrac{\ddot{E}}{K_a} + \dfrac{\dddot{E}}{K_j} + N_{E_m} \end{cases} \tag{a11}$$

$$\begin{cases} \Delta R_j = R_r - R_m = a_0 + a_1 \dot{R}_j + a_2 \sec E_j + N_j \\ \Delta A_j = A_r - A_m = b_0 + b_1 \dot{A}_j + b_2 \ddot{A}_j + b_3 \sin A_j \tan E_j + b_4 \cos A_j \tan E_j + b_5 \tan E_j + b_6 \sec E_j + N_j \\ \Delta E_j = E_r - E_m = c_0 + c_1 \dot{E}_j + c_2 \ddot{E}_j + c_3 \sin A_j + c_4 \cos A_j + c_5 \cos E_j + c_6 \cot E_j + N_j \end{cases} \tag{a12}$$

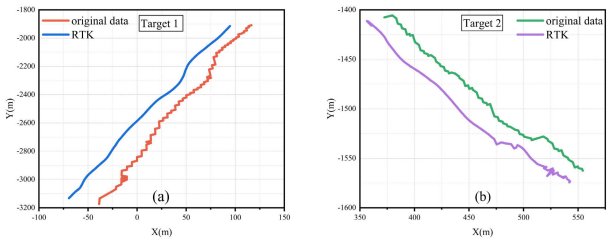

FIGURE 12. Trajectory of a single target. (a) Target 1; (b) Target 2.

The undefined parameters were estimated using the least squares method. Equation (a12) was transformed to obtain the second-order fitting system error correction equation as follows:

$$\begin{cases} A = (O^T O)^{-1} O^T \Delta R' \\ B = (P^T P)^{-1} P^T \Delta A' \\ C = (Q^T Q)^{-1} Q^T \Delta E' \end{cases} \tag{a16}$$

Equation was calculated to obtain the original parameter matrix of the second-order fitting system error model. Equations (a12)-(a15) were substituted into (a16) to calculate the actual parameters of the model according to their definitions in the matrices X and Y. The model is subsequently constructed.

APPENDIX B
ESTABLISHMENT PROCESS OF DATASETS

Datasets were simply established as follows:

(i) Temporal alignment of original data: The original data are processed using the method discussed above.

(ii) Trajectory drafting: The data collected by radar and RTK were coordinate transformed to obtain the three-dimensional coordinates in the rectangular coordinate system. Subsequently, the drawing tool of MATLAB was used to draft trajectories. A segment of measured data was taken as an example to draft trajectories as shown in Fig. 12.

(iii) Data segmentation: measured data were segmented based on the drafted trajectory of double targets. The data of double targets were recorded separately and simultaneously in rectilinear and curved motions.

(iv) Connection of data point traces: based on the results of data segmentation, data segments are correspondingly connected to generate datasets.

REFERENCES

[1] L. Lijun, T. Guoyong, Z. Shiyin, and L. Xi, "High precision estimation and separation method of external measurement data error," *Radar Sci. Technol.*, vol. 18, no. 6, pp. 605–610, 2020.

[2] D. Goshen-Meskin and I. Y. Bar-Itzhack, "Unified approach to inertial navigation system error modeling," *J. Guid., Control, Dyn.*, vol. 15, no. 3, pp. 648–653, May 1992.

[3] D. L. McCann and P. S. Bell, "A simple offset 'calibration' method for the accurate geographic registration of ship-borne X-band radar intensity imagery," *IEEE Access*, vol. 6, pp. 13939–13948, 2018, doi: 10.1109/ACCESS.2018.2814081.

[4] Z. Wei, L. Peng, and W. Jun, "Analysis and suppression of radial velocity estimation error for moving targets in wideband LFMCW radar," *J. Beijing Univ. Aeronaut. Astronaut.*, 2023, doi: 10.13700/j.bh.1001-5965.2023.0689.

[5] J. Guo, Q. Xu, and H. Liu, "Design and implementation of radar calibration for pulse instrumentation based on differential BDS techniques," *J. Ordnance Equip. Eng.*, vol. 43, pp. 139–144, 2022.

[6] B. Zhang, D. Ji, S. Liu, W. Xu, and X. Zhu, "Autonomous underwater vehicle navigation: A review," *Ocean Eng.*, vol. 273, Apr. 2023, Art. no. 113861.

[7] M. Cai, G. Wu, and Y. Yao, "Bi/multi-static corporative positioning and tracking," *Modern Radar*, vol. 44, pp. 75–81, 2022.

[8] G. Li, G. Li, and Y. He, "Distributed multiple resolvable group targets tracking based on hypergraph matching," *IEEE Sensors J.*, vol. 23, no. 9, pp. 9669–9676, May 2023.
[9] Y. Dong, G. Huang, and B. Li, "A multi-radar error registration algorithm based on TSSH-EKF," *J. Ordnance Equip. Eng.*, vol. 41, pp. 71–75, 2020.
[10] Y. Dong and G. Huang, "A multi-radar error registration algorithm based on SSR-TSEKF," *Electron. Opt. Control*, vol. 27, pp. 27–31, 2020.
[11] G. Huang and Y. Dong, "Auxiliary radar time-varying system error estimation method based on weighted limited memory," *Ship Electron. Eng.*, vol. 41, pp. 40–45, 2021.
[12] P. Z. Peebles, "Further results on multipath angle error reduction using multiple-target methods," *IEEE Trans. Aerosp. Electron. Syst.*, vol. AES-9, no. 5, pp. 654–659, Sep. 1973, doi: 10.1109/TAES.1973.309747.
[13] S. Haoran, L. Faxing, Q. Jiangxin, and Y. Guang, "Cooperative target tracking of UAVs based on aided beacon," *Syst. Eng. Electron.*, vol. 44, no. 7, pp. 2302–2310, 2022.
[14] S. Haoran, L. Faxing, W. Hangyu, and X. Junfei, "Cooperative control and collision avoidance for two UAVs based on optimization of observation," *Control Decision*, vol. 37, no. 3, pp. 593–604, 2022.
[15] F. Jinbo, Z. Dong, W. Mengyang, and Z. Junmin, "Unmanned aerial vehicle trajectory planning method for enhancing target localization accuracy," *Acta Armamentarii*, vol. 44, no. 11, pp. 1–13, Nov. 2023. [Online]. Available: http://kns.cnki.net/kcms/detail/11.2176.tj.20231103.1452.004.html, doi: 10.12382/bgxb.2023.0776.
[16] X. Zhou, Y. Zhang, and X. Zhao, "Joint target localization and sensor registration under multi-source range measurements," *Command Inf. Syst. Technol.*, vol. 12, no. 70, pp. 70–74, 2021.
[17] Q. Dai and F. Lu, "A new spatial registration algorithm of aerial moving platform to sea target tracking," *Sensors*, vol. 23, no. 13, p. 6112, Jul. 2023.
[18] G. Huang and Y. Dong, "ECEF-based two-stage extended Kalman filter error registration method," *Ship Electron. Eng.*, vol. 40, no. 8, p. 6, 2020.
[19] Y. Dong, Y. Zhang, S. Xia, and W. Jiang, "Real-time error registration algorithm for tracking target maneuvering," *Electron. Opt. Control*, nos. 1–8, pp. 1–8, 2022. [Online]. Available: http://kns.cnki.net/kcms/detail/41.1227.TN.20220622.1117.002.html
[20] D. Yunlong, H. Gaodong, L. Baozhu, Z. Lin, and G. Jian, "Error analysis of sea radar system based on AIS auxiliary information," *Modern Radar*, vol. 42, no. 5, pp. 21–27, 2020.
[21] G. E. Pollon and G. W. Lank, "Angular tracking of two closely spaced radar targets," *IEEE Trans. Aerosp. Electron. Syst.*, vol. AES-4, no. 4, pp. 541–550, Jul. 1968, doi: 10.1109/TAES.1968.5409022.
[22] P. Z. Peebles, "Multipath angle error reduction using multiple-target methods," *IEEE Trans. Aerosp. Electron. Syst.*, vol. AES-7, no. 6, pp. 1123–1130, Nov. 1971, doi: 10.1109/TAES.1971.310213.
[23] Z. Tianshu and L. Yinlong, "Track association algorithm of system error correction based on peer-to-peer structure," *Modern Radar*, vol. 44, no. 1, pp. 65–70, 2022.
[24] W. Wenkang, F. Jingan, S. Bao, and L. Xinxin, "Vehicle state estimation using interacting multiple model based on square root cubature Kalman filter," *Appl. Sci.*, vol. 11, no. 22, p. 10772, Nov. 2021.
[25] G. A. Shah, S. Khan, S. A. Memon, M. Shahzad, Z. Mahmood, and U. Khan, "Improvement in the tracking performance of a maneuvering target in the presence of clutter," *Sensors*, vol. 22, no. 20, p. 7848, Oct. 2022.
[26] H. Li, L. Yan, and Y. Xia, "Distributed robust Kalman filtering for Markov jump systems with measurement loss of unknown probabilities," *IEEE Trans. Cybern.*, vol. 52, no. 10, pp. 10151–10162, Oct. 2022.

YUXIANG ZHOU was born in 2001. He received the B.S. degree in fire command and control engineering from the Naval University of Engineering, in 2023, where he is currently pursuing the master's degree. His current research interests include combat systems and information engineering.

FAXING LU was born in 1974. He received the B.S. degree in mine and anti-mine and the M.S. degree in systems engineering from the Naval University of Engineering, in 1997 and 2000, respectively, and the Ph.D. degree in weapon and military technology, military applications and systems from Kuznetsov Naval Academy, Russia, in 2008. He is currently a Professor with the Naval University of Engineering. His current research interests include advanced weapon control and multi-agent cooperative control.

QIUYANG DAI was born in 1999. He received the B.S. degree in command and control engineering from the Naval University of Engineering, in 2021, where he is currently pursuing the master's degree. His current research interests include combat systems and information engineering.

JUNFEI XU was born in 1990. He received the B.S. degree in fire command and control engineering and the M.S. and Ph.D. degrees in systems engineering from the Naval University of Engineering, in 2013 and 2019, respectively. He is currently a Lecturer with the Naval University of Engineering. His current research interest includes the assessment of operational effectiveness of naval weapons.